

Integer and fractional Talbot effect of Walsh functions in a tapered gradient-index medium

OSVALDO TRABOCCHI[†] and CARLOS GÓMEZ-REINO[‡]

Optics Laboratory, Applied Physics Department, Faculty of Physics and Optics and Optometry School, University of Santiago de Compostela, Campus Sur, E15782 Santiago de Compostela, Spain[§]
e-mails: [†]faosvald@usc.es; [‡]facgrc@usc.es
[§]website <http://www.usc.es/grinteam>

(Received 12 May 2003; revision received 18 June 2003)

Abstract. The complex amplitude distribution for a Gaussian illumination in a tapered gradient-index medium when the input signal is a binary Walsh function is considered. The integer and fractional Talbot effect is studied and the analysis is extended to more general signals by the completeness of the Walsh functions set. Analogies with the conventional lens-imaging formula are found.

1. Introduction

The integer and fractional Talbot effect is a phenomenon widely studied in optics and has important technical applications [1, 2]. This effect has been generalized to the propagation through a tapered gradient index medium for nonuniform and uniform illumination in recent papers [3, 4].

Moreover, the Walsh functions [5] have been efficiently applied to some problems related to the Talbot effect in free propagation [6, 7]. It is known that the spatial periodicity of an aperture is a sufficient condition for originating self-images, but it has been demonstrated that the Walsh functions, being in general not periodical functions, obey the Talbot effect in free propagation under specific conditions [8]. The importance of the study of the properties of the Walsh functions is based on the fact that they form a complete set of functions, and this allows the extension of the results to more general expansions.

In this paper we analyse the evolution of the propagated field for nonuniform illumination when a Walsh function is located at the input of a tapered GRIN medium. The conditions for the performance of the integer and fractional Talbot effect are found. The study could be extended to more general signals. Moreover, an analogy between the self-image effect of the Walsh and the Rademacher functions and the conventional lens-imaging formula is achieved.

2. Propagation of a Walsh function in a GRIN media

The refractive index of a tapered GRIN medium characterized by a transverse parabolic refractive index modulated by an axial index is given by

$$n^2(x, z) = n_0^2[1 - g^2(z)x^2], \quad (1)$$

where n_0 is the index at the z optical axis and $g(z)$ is the taper function that describes the evolution of the transverse index along the z axis.

Let us consider that at the input of this medium is located a one-dimensional finite object of spatial dimension ξ and transmittance

$$T(x_0) = \frac{1}{2}[1 + \text{Wal}_N(x_0)] = W_N(x_0), \quad (2)$$

where $W_N(x_0)$ is the binary expression of a Walsh function $\text{Wal}_N(x_0)$ of ordering integer number or index $N \geq 0$ [5]. The Walsh functions $\{\text{Wal}_N(x_0)\}$ are a series of bivalued square-wave functions and form a complete set of orthogonal functions. Inside a finite domain $|x_0| \leq \xi/2$ they can be defined as

$$\text{Wal}_N(x_0) = \prod_{r=p}^m [R_r(x_0)]^{g_r}, \quad (3)$$

where $[R_r(x_0); r = 0, 1, 2, \dots]$ are the Rademacher functions, which are periodic square waves of amplitude ± 1 and form an incomplete set of orthogonal functions. The integers m , p , and g_r are defined by the binary expansion of N : $N = \sum_{r=p}^m g_r 2^r$, where g_r are the corresponding bits: 0 or 1. The Rademacher functions have a period d_r that rises with their ordering number or index r

$$d_r = \xi 2^{1-r}, \quad (4)$$

and they can be expressed by [9] as

$$R_r(t) = \text{sign} \left[\cos \left(2^r \pi \frac{t}{\xi} \right) \right], \quad (5)$$

if the domain is $t \in [0; \xi]$. However, if the domain is $x_0 \in [-\xi/2; \xi/2]$, the translation $x_0 = t - (\xi/2)$ can be introduced to preserve their shapes and properties. Therefore, they will take the form

$$R_r(x_0) = \text{sign} \left\{ \cos \left[2^r \pi \left(\frac{x_0}{\xi} + \frac{1}{2} \right) \right] \right\}. \quad (6)$$

Insertion of equation (3) into equation (2) and substitution of the Rademacher functions by their corresponding Fourier expansions gives

$$T(x_0) = \frac{1}{2} \left\{ 1 + \prod_{r=p}^m \left[\sum_{k_r=-\infty}^{+\infty} c_{k_r} \exp \left(2\pi i x_0 \frac{k_r}{d_r} \right) \right]^{g_r} \right\} \text{rect} \left(\frac{x_0}{\xi} \right), \quad (7)$$

where c_{k_r} is the amplitude of the k th harmonic in the expansion of $R_r(x_0)$, and the rect function confines the series to the strict definition of the finite aperture of dimension ξ .

When the hybrid optical structure formed by the one-dimensional object and the tapered GRIN medium is illuminated by a coherent nonuniform beam (figure 1), the complex amplitude distribution at $z = 0$ will be

$$\phi(x_0) = T(x_0)\psi_0(x_0), \quad (8)$$

where

$$\psi_0(x_0) = \left[\frac{w_0}{w(0)} \right]^{1/2} \exp[i\varphi(0)]\psi[x_0; U(0)], \quad (9)$$

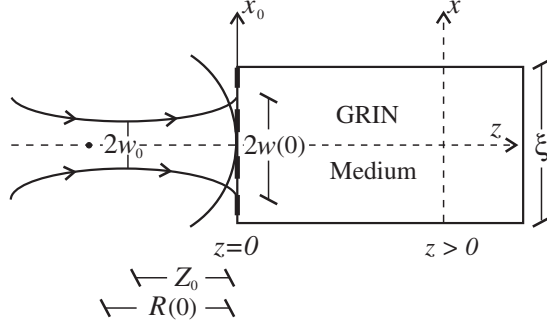


Figure 1. Geometry of a tapered GRIN medium with a bivalued aperture illuminated by a Gaussian beam.

is the complex amplitude distribution due to a Gaussian illumination of wavelength λ , and

$$\psi[x_0; U(0)] = \exp\left[i\frac{\pi U(0)x_0^2}{\lambda}\right], \quad (10)$$

is the quadratic phase factor of the cylindrical Gaussian beam. The beam parameters at distance Z_0 from the waist plane of diameter $2w_0$ are given by the complex curvature U and the on-axis phase φ , that is

$$U(0) = \frac{1}{R(0)} + i\frac{\lambda}{\pi w_0^2}, \quad (11)$$

and

$$\varphi(0) = \tan^{-1}\left(\frac{\lambda Z_0}{\pi w_0^2}\right), \quad (12)$$

where $R(0)$ and $w(0)$ are the radius of curvature and the half-width at $z=0$, respectively.

The field distribution in the tapered GRIN medium at $z > 0$ is given by the integral equation [10]

$$\phi(x; z) = \int_{-\infty}^{+\infty} \phi(x_0)K(x, x_0; z)dx_0, \quad (13)$$

where K is the one-dimensional optical propagator of this medium expressed as

$$K(x, x_0; z) = \left[\frac{n_0}{i\lambda H_1(z)}\right]^{1/2} \exp\left(i\frac{2\pi}{\lambda}n_0 z\right) \exp\left\{i\frac{\pi n_0}{\lambda H_1(z)}\left[x^2 \dot{H}_1(z) + x_0^2 H_2(z) - 2xx_0\right]\right\}, \quad (14)$$

where H_1 , H_2 and \dot{H}_1 , \dot{H}_2 are the position and the slope of the axial and field rays at z , respectively, and the dot denotes a derivative with respect to z .

Substituting equations (7) to (10) and (14) into equation (13) and integrating we find

$$\begin{aligned} \phi(x; z) = & \frac{1}{2} \left(C + \left[\frac{w_0}{w(0)G(z)} \right]^{1/2} \exp[i\varphi(z)] \exp \left[i \frac{\pi U(z)}{\lambda} x^2 \right] \right. \\ & \times \sum_{k_p=-\infty}^{+\infty} \dots \sum_{k_m=-\infty}^{+\infty} \left\{ c_{k_p} \dots c_{k_m} \exp \left[-i \frac{\pi \lambda H_1(z)}{n_0 G(z)} \left(\sum_{r=p}^m \frac{g_r k_r}{d_r} \right)^2 \right] \right. \\ & \left. \left. \times \exp \left[i \frac{2\pi}{G(z)} \sum_{r=p}^m \frac{g_r k_r}{d_r} x \right] \right\} \right), \end{aligned} \quad (15)$$

where $U(z)$ denotes the complex curvature of the Gaussian beam at z given by

$$U(z) = n_0 \dot{G}(z) G^{-1}(z) = n_0 \frac{d[\ln G(z)]}{dz}, \quad (16)$$

with $G(z)$ and $\dot{G}(z)$ being

$$G(z) = \frac{U(0)H_1(z)}{n_0} + H_2(z), \quad (17a)$$

$$\dot{G}(z) = \frac{U(0)\dot{H}_1(z)}{n_0} + \dot{H}_2(z), \quad (17b)$$

and $\varphi(z)$ indicates the on-axis phase at z

$$\varphi(z) = \varphi(0) + \frac{2\pi}{\lambda} n_0 z. \quad (18)$$

The factor C in equation (15) comes from the propagation of the function $\text{rect}(x_0/\xi)$ through the tapered gradient index medium and can be considered a constant factor compared with the variation of the diffracted field of the Walsh function. To arrive at equation (15) we have supposed that

$$2^p \gg 1, \quad (23)$$

in order to minimize the effect of the finite size of $W_N(x_0)$ on $\phi(x; z)$. This condition selects a sub-set of Walsh functions whose Rademacher functions are tight enough.

Equation (15) represents the propagation of the Walsh function diffraction orders through the tapered GRIN medium.

3. Imaging condition

The second exponential term of the summation in equation (15) has a fundamental significance for the analysis of the self-image phenomenon, as we will show. Even more, when this term becomes unity the field obeys the imaging condition. Let us consider the axial distance $z = z_q$ in the tapered GRIN media,

where q is an integer, such that when $H_1(z_q) = 0$, equation (15) reduces to

$$\begin{aligned} \phi(x; z_q) = & \frac{1}{2} \left\{ C + \left(\frac{w_0}{w(z_q)} \right)^{1/2} \exp[i\varphi(z_q)] \exp \left[i \frac{\pi U(z_q)}{\lambda} x^2 \right] \right. \\ & \left. \times \sum_{k_p=-\infty}^{+\infty} \dots \sum_{k_m=-\infty}^{+\infty} c_{k_p} \dots c_{k_m} \exp \left[i 2\pi \sum_{r=p}^m \frac{g_r k_r}{d_r(z_q)} x \right] \right\}, \end{aligned} \quad (20)$$

where the beam half-width, the complex curvature, and the periods of the images of each $R_r(x_0)$ at z_q are given, respectively, by

$$w(z_q) = w(0)H_2(z_q), \quad (21)$$

$$U(z_q) = U(0) \frac{\dot{H}_1(z_q)}{H_2(z_q)}, \quad (22)$$

and

$$d_r(z_q) = d_r H_2(z_q), \quad r = p, \dots, m. \quad (23)$$

The complex amplitude distribution at z_q is then a magnified replica of the complex amplitude distribution at $z = 0$, except for a constant phase factor, as it can be observed when comparing equation (20) with equation (8) and using equations (7), (9), and (10).

4. Integer Talbot effect for a Walsh function

In addition to the above self-imaging phenomenon, a periodic repetition along the z axis of the field distribution occurs for the Talbot condition. The summation in equation (15) can be rewritten as

$$\begin{aligned} \phi(x; z_q) \propto & \sum_{k_p=-\infty}^{+\infty} \dots \sum_{k_m=-\infty}^{+\infty} \left(c_{k_p} \dots c_{k_m} \exp \left\{ \frac{\pi \lambda \operatorname{Im}[G(z)]}{n_0 |G(z)|^2} H_1(z) \left(\sum_{r=p}^m \frac{g_r k_r}{d_r} \right)^2 \right\} \right. \\ & \times \exp \left\{ \frac{2\pi \operatorname{Im}[G(z)]}{|G(z)|^2} \left(\sum_{r=p}^m \frac{g_r k_r}{d_r} \right) x \right\} \times \exp \left\{ i \frac{\pi \lambda \operatorname{Re}[G(z)]}{n_0 |G(z)|^2} H_1(z) \left(\sum_{r=p}^m \frac{g_r k_r}{d_r} \right)^2 \right\} \\ & \left. \times \exp \left\{ i \frac{2\pi \operatorname{Re}[G(z)]}{|G(z)|^2} \left(\sum_{r=p}^m \frac{g_r k_r}{d_r} \right) x \right\} \right), \end{aligned} \quad (24)$$

where $\operatorname{Re}[G(z)]$ and $\operatorname{Im}[G(z)]$ are the real and imaginary parts of $G(z)$

$$\operatorname{Re}[G(z)] = \frac{H_1(z)}{n_0 R(0)} + H_2(z), \quad (25)$$

$$\operatorname{Im}[G(z)] = \frac{H_1(z)}{z_R}, \quad (26)$$

and z_R is the Rayleigh range that characterizes the Lorentzian profile of the Gaussian beam intensity along the z axis of the GRIN medium, and is expressed as

$$z_R = \frac{\pi n_0 w^2(0)}{\lambda}, \quad (27)$$

and $|G(z)|$ is the modulus of $G(z)$, that is

$$|G(z)| = \left\{ \left[\frac{H_1(z)}{n_0 R(0)} + H_2(z) \right]^2 + \frac{H_1^2(z)}{z_R^2} \right\}^{1/2}, \quad (28)$$

which relates the beam half-width at $z > 0$ to the beam half-width at $z = 0$ as follows

$$w(z) = w(0)|G(z)|. \quad (29)$$

The first two exponential terms and the next two phase terms of equation (24) describe the amplitude and phase changes of the diffraction orders along the axial and the transverse directions, respectively. In particular, the third term represents the phase changes of the diffraction orders with axial distance z .

The third exponential term in equation (24) for a given Rademacher function $R_j(x_0) \subset W_N(x_0)$ can be expressed as

$$\exp \left\{ i \frac{\pi \lambda \operatorname{Re}[G(z)]}{n_0 |G(z)|^2} H_1(z) \left[\left(\frac{k_j}{d_j} \right)^2 + 2 \frac{k_j}{d_j} \sum_{r \neq j}^m \frac{g_r k_r}{d_r} \right] \right\}. \quad (30)$$

All diffraction orders due to $R_j(x_0)$ will be in, or opposite phase at a length z_{v_j} when this term becomes $+1$ or -1 respectively. This happens whenever

$$\frac{\operatorname{Re}[G(z_{v_j})]}{n_0 |G(z_{v_j})|^2} H_1(z_{v_j}) = v_j \frac{d_j^2 2^{j-p}}{\lambda}, \quad (31)$$

where v_j is a positive integer. In this case, the last term of equation (24) describes, for $r = j$, the phase changes of the diffraction orders of $R_j(x_0)$ along the transverse direction and under condition (31) can be written as

$$\exp \left\{ i \frac{2\pi \operatorname{Re}[G(z_{v_j})] k_j}{n_0 |G(z_{v_j})|^2} \frac{k_j}{d_j} x \right\} = \exp \left[i \frac{2\pi k_j}{d_j(z_{v_j})} x \right], \quad (32)$$

where

$$d_j(z_{v_j}) = d_j M(z_{v_j}), \quad (33)$$

and

$$M(z_{v_j}) = \frac{|G(z_{v_j})|^2}{\operatorname{Re}[G(z_{v_j})]} = \frac{w^2(z_{v_j})}{w^2(0) \operatorname{Re}[G(z_{v_j})]}, \quad (34)$$

with equation (29) being used. The complex amplitude distribution in z_{v_j} reproduces then the magnified self-images of $R_j(x_0)$, with the period and transverse magnifications given by equations (33) and (34), respectively. Self-images of $R_j(x_0)$ at z_{v_j} are spatially modulated by diffraction orders due to the remaining Rademacher functions. Therefore, equation (31) can be called the integer Talbot condition for $R_j(x_0)$ including in $W_N(x_0)$ in a GRIN media under Gaussian illumination where v_j is an integer referred to as the self-image number. If v_j is even, the field will correspond to positive self-images of $R_j(x_0)$, and if v_j is odd, negative self-images of $R_j(x_0)$ are obtained.

Likewise, from equations (4) and (31), a recursion Talbot condition between Rademacher functions can be found. For instance, for $R_j(x_0)$ and $R_k(x_0)$ in

$W_N(x_0)$, with $p \leq j, h \leq m$, and supposing that $z_{v_j} = z_{v_h}$, we can write that

$$v_h = 2^{h-j}v_j. \quad (35)$$

Therefore, if $j < h$, the first self-image of $R_j(x_0)$ coincides with the $v_h = 2^{h-j}$ -th self-image of $R_h(x_0)$, or in general, at the place where $R_j(x_0)$ focuses, all $R_h(x_0)$ with $p \leq h \leq m$ are also reproduced. This self-image superposition will be in general spatially modulated by the remaining defocused Rademacher functions $R_h(x_0)$, with $h < j$, which act as a noise source, except when $2^{h-j}v_j$ is an integer number, in such case $R_h(x_0)$ focuses too. In particular, at the distances where $R_p(x_0)$ has its self-images, all the Rademacher functions $R_j(x_0) \subset W_N(x_0)$ are also focused, the Talbot distance of $R_p(x_0)$ then coincides with the Talbot distance of $W_N(x_0)$, and equation (31) becomes

$$\frac{\text{Re}[G(z_v)]}{n_0|G(z_v)|^2} H_1(z_v) = \nu \frac{d_p^2}{\lambda}, \quad (36)$$

where $\nu = \nu_p$ is a positive integer, and $z_\nu = z_{\nu_p}$ is the self-image distance of $W_N(x_0)$. These self-images will be generated by the product of the Rademacher functions $R_j(x_0) \subset W_N(x_0)$. Equation (36) predicts the location of positive and negative self-images of $W_N(x_0)$, when ν is even or odd, respectively. From equation (35), we can observe that if ν_p is an integer, ν_j is even for all j with $p < j \leq m$, then, at these Talbot distances z_ν , while the remaining Rademacher functions in the product of $W_N(x_0)$ focus only positively, the Rademacher function $R_p(x_0)$ forms its positive or negative images producing the positive or negative self-images of $W_N(x_0)$, respectively. The magnification of these images is expressed by equation (34) for $j = p$. In short, $R_p(x_0)$ governs the self-imaging evolution of $W_N(x_0)$.

5. Fractional Talbot effect for a Walsh function

The analysis of equation (30) also indicates that there are self-images at fractions of the integer Talbot distances where the phase differences between diffraction orders of $R_j(x_0)$ are not integer. The condition for the fractional Talbot effect can be written as

$$\frac{\text{Re}[G(z_{\alpha_j/\beta_j})]}{n_0|G(z_{\alpha_j/\beta_j})|^2} H_1(z_{\alpha_j/\beta_j}) = \frac{\alpha_j d_j^2 2^{j-p}}{\beta_j \lambda}, \quad (37)$$

where α_j and β_j are co-prime positive integers. The complex amplitude distribution at planes z_{α_j/β_j} , is periodically repeated along the optical axes and in this case, the recursion formulas for Rademacher functions in $W_N(x_0)$, will be expressed as

$$\frac{\alpha_h}{\beta_h} = 2^{h-j} \frac{\alpha_j}{\beta_j}, \quad (38)$$

in which equations (4) and (37) have been used. Then, at z_{α_j/β_j} where $R_j(x_0)$ has its fractional self-image α_j/β_j , any $R_h(x_0) \subset W_N(x_0)$ has its fractional self-image as $\alpha_h/\beta_h = 2^{h-j}\alpha_j/\beta_j$. Moreover, in the particular case where z is an integer Talbot distance for $R_j(x_0)$, the Rademacher functions $R_h(x_0)$ with $j \leq h \leq m$ will have integer self-images, while the functions $R_h(x_0)$ with $p \leq h \leq j$ will have, in general, fractional self-images, except when $2^{h-j}\alpha_j/\beta_j$ is an integer.

The condition for the fractional self-images of $W_N(x_0)$ will be the same as that obeyed by $R_p(x_0)$

$$\frac{\operatorname{Re}[G(z_{\alpha/\beta})]}{n_0|G(z_{\alpha/\beta})|^2} H_1(z_{\alpha/\beta}) = \frac{\alpha d_p^2}{\beta \lambda}, \quad (39)$$

where $\alpha = \alpha_p$ and $\beta = \beta_p$ are co-prime integers, and $z_{\alpha/\beta} = z_{\alpha_p/\beta_p}$ is the fractional self-image distance of $W_N(x_0)$. A similar expression to equation (34) for the magnification of the fractional self-images of $R_j(x_0)$ and $W_N(x_0)$ can be easily obtained.

Likewise, from equations (4), (31), and (39), we find that for the for Walsh function

$$\frac{\alpha}{\beta} = \frac{v_j}{2^{j-p}}, \quad (40)$$

and it follows that all the integer self-images v_j of $R_j(x_0) \subset W_N(x_0)$ coincide with a fractional self-image $\alpha/\beta = v_j/2^{j-p}$ of $W_N(x_0)$. Moreover, when all these Rademacher functions have an integer self-image, $W_N(x_0)$ has an integer self-image too, given by product of the functions as in equation (3).

A more general relation can be found from equations (37) and (39):

$$\frac{\alpha}{\beta} = \frac{\alpha_j}{2^{j-p}\beta_j}, \quad (41)$$

At the distances $z_{\alpha/\beta}$, where $W_N(x_0)$ has its fractional self-image α/β , the Rademacher function $R_j(x_0) \subset W_N(x_0)$ has its fractional self-image $\alpha_j/2^{j-p}\beta_j$. In other words, the fractional self-images α/β of $W_N(x_0)$ are a product of the fractional self-images of all $R_j(x_0) \subset W_N(x_0)$, of orders $\alpha_j/2^{j-p}\beta_j$.

For illustrating these results we consider a Walsh function represented by $W_{896}(x_0) = R_7(x_0)R_8(x_0)R_9(x_0)$, with $p = 7$, that obeys condition (19). From equation (41), the relationship between the fractional self-image orders α/β of $W_{896}(x_0)$ and the fractional self-image orders α_j/β_j of $R_j(x_0)$, with $j = 7, 8$ and 9 , at the distance $z_{\alpha/\beta}$, is

$$\frac{\alpha}{\beta} = \frac{\alpha_7}{\beta_7} = \frac{\alpha_8}{2\beta_8} = \frac{\alpha_9}{4\beta_9}. \quad (42)$$

Table 1 shows different fractional orders of $W_{896}(x_0)$, $R_7(x_0)$, $R_8(x_0)$, and $R_9(x_0)$. Each column represents the self-image orders α/β of $W_{896}(x_0)$ and the corresponding orders α_j/β_j of its constituting Rademacher functions, at distances $z_{\alpha/\beta}$ increasing with α/β from the left to the right. From the first column we notice that the self-image $1/8$ of $W_{896}(x_0)$ is equal to the product of the self-images $1/8$ of $R_7(x_0)$, $1/4$ of $R_8(x_0)$, and $1/2$ of $R_9(x_0)$. Note that $R_9(x_0)$ is the first function to produce an integer negative self-image (2nd column), $R_8(x_0)$ (4th column) coincides with a positive integer self-image for $R_9(x_0)$, and finally $R_7(x_0)$ and $W_{896}(x_0)$ (8th column) coincide with the first and second positive integer self-images of $R_8(x_0)$ and $R_9(x_0)$, respectively. The 16th column represents the first positive self-image of the Walsh function. Moreover, taking $j = 4$ as reference, we observe that where $R_8(x_0)$ focuses (i.e., it has an integer self-image), its superior index $R_9(x_0)$ focuses too, while its inferior index $R_7(x_0)$ does not focus (it has a fractional

self-image), except when $2^{h-j}v_h = 2^{7-8}v_8$ is an integer number, as we have predicted previously.

6. Equivalent multifocal lens

An interesting analogy between the Talbot condition and the conventional lens formula can be obtained if equation (37) is written as

$$\frac{2^{j-p}\alpha_j d_j^2}{\beta_j \lambda D_{0j}} = \frac{1}{R(0)} - \frac{1}{z'_{\alpha_j/\beta_j}}, \quad (43)$$

where

$$z'_{\alpha_j/\beta_j} = R(0) + z_{\alpha_j/\beta_j} = \frac{|G(z_{\alpha_j/\beta_j})|^2}{\text{Re}[G(z_{\alpha_j/\beta_j})]} R(0), \quad (44)$$

$$D_{0j}^2 = \frac{H_1(z_{\alpha_j/\beta_j})}{n_0 z_{\alpha_j/\beta_j}} R^2(0), \quad (45)$$

and

$$z_{\alpha_j/\beta_j} = \frac{|G(z_{\alpha_j/\beta_j})|^2 - \text{Re}[G(z_{\alpha_j/\beta_j})]}{\text{Re}[G(z_{\alpha_j/\beta_j})]} R(0). \quad (46)$$

Therefore, equation (43) can be regarded as the equation of an equivalent lens of multi-focal distance

$$f_{\alpha_j/\beta_j} = \frac{\beta_j \lambda D_{0j}}{2^{j-p}\alpha_j d_j^2}, \quad (47)$$

situated at the curvature center of the Gaussian beam that illuminates the periodic object $R_j(x_0)$ as shown in figure 2. The lateral magnification of this equivalent lens can be expressed as

$$M_t(z_{\alpha_j/\beta_j}) = \frac{z'_{\alpha_j/\beta_j}}{R(0)} = \frac{|G(z_{\alpha_j/\beta_j})|^2}{\text{Re}[G(z_{\alpha_j/\beta_j})]} = \frac{w^2(z_{\alpha_j/\beta_j})}{w^2(0) \text{Re}[G(z_{\alpha_j/\beta_j})]}, \quad (48)$$

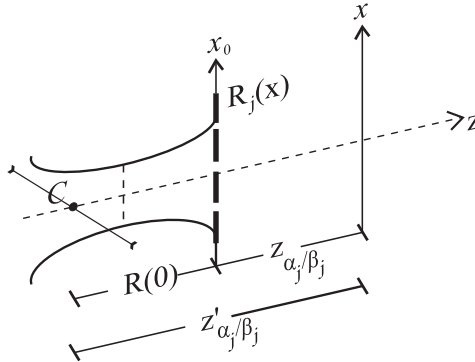


Figure 2. Equivalent optical system for the self-image effect in a tapered GRIN medium under Gaussian illumination. Here we have taken the contribution of only one of the Rademacher functions in the Walsh function aperture.

where z'_{α_j/β_j} and $R(0)$ are the image and object distances, respectively. Equation (48) coincides with equation (34). This analysis is valid for every $R_j(x_0) \subset W_N(x_0)$, and similar results can be found for the Walsh function $W_N(x_0)$, starting from equation (39) or replacing $j = p$ in equations (43) to (48).

7. Talbot distances

The axial localization of self-images can be also obtained from the Talbot condition if we take into account that the axial and field rays are given by [10]

$$H_1(z) = [g_0 g(z)]^{-1/2} \sin \left[\int_0^z g(z') dz' \right], \quad (49a)$$

and

$$H_2(z) = \left[\frac{g_0}{g(z)} \right]^{1/2} \cos \left[\int_0^z g(z') dz' \right], \quad (49b)$$

where g_0 is the value of $g(z)$ at $z = 0$. They are now expressed as

$$H_1(z) = \frac{u(z)}{\{g_0 g(z)[1 + u^2(z)]\}^{1/2}}, \quad (50a)$$

and

$$H_2(z) = \left\{ \frac{g_0}{g(z)[1 + u^2(z)]} \right\}^{1/2}, \quad (50b)$$

where

$$u(z) = \tan \left[\int_0^z g(z') dz' \right]. \quad (51)$$

Substituting equation (50) into equation (37), we obtain

$$au^2(z_{\alpha_j/\beta_j}) + bu(z_{\alpha_j/\beta_j}) + c = 0, \quad (52)$$

where

$$a = \frac{1}{g_0} \left\{ \frac{\alpha_j}{\beta_j} d_j 2^{j-p} n_0 \left[\frac{1}{n_0^2 R^2(0)} + \frac{1}{z_R^2} \right] - \frac{1}{n_0 R(0)} \right\}, \quad (53)$$

$$b = 2 \frac{\alpha_j d_j^2 2^{j-p}}{\beta_j R(0)} - \lambda, \quad (54)$$

and

$$c = \frac{\alpha_j}{\beta_j} d_j^2 2^{j-p} n_0 g_0. \quad (55)$$

The solution of equation (52) is given by

$$u(z_{\alpha_j/\beta_j}) = \frac{n_0 g_0 R^2(0) z_R^2 \lambda}{2(\alpha_j/\beta_j) d_j^2 2^{j-p} [z_R^2 + n_0^2 R^2(0)] - 2\lambda R(0) z_R^2} \times \left[1 - \frac{2\alpha_j d_j^2 2^{j-p}}{\beta_j R(0) \lambda} - \sqrt{1 - \left(\frac{2n_0 \alpha_j d_j^2 2^{j-p}}{\beta_j z_R \lambda} \right)^2} \right]. \quad (67)$$

We have chosen the negative sign of the square root in equation (56) since it permits the initial condition $u(z_{\alpha_j/\beta_j}) = 0$ to be obeyed for $\alpha_j/\beta_j = 0$, which indicates the position of the object at the input.

From equation (56) it follows that real values of $u(z_{\alpha_j/\beta_j})$ are achieved when the requirement

$$\frac{2n_0 \alpha_j d_j^2 2^{j-p}}{\beta_j z_R \lambda} \leq 1, \quad (57)$$

or

$$\frac{\alpha_j}{\beta_j} \leq \frac{\pi}{2^{j-p+1}} \left(\frac{w(0)}{d_j} \right)^2, \quad (58)$$

is fulfilled, which makes use of equation (27).

Then the fraction α_j/β_j is limited by a square relationship between the beam half-width at $z = 0$ and the period of the Rademacher function. One or more self-images are obtained as $w(0)/d_j \geq \sqrt{2^{j-p+1}/\pi}$.

Likewise, equation (56) includes uniform illumination as a special case. For this illumination $R(0) \rightarrow Z_0$, $w(0) \rightarrow \infty$ and $z_R \rightarrow \infty$, Z_0 being the curvature radius of the uniform wave at the input. Under these conditions, equation (56) reduces to

$$u(z_{\alpha_j/\beta_j}) = \frac{(\alpha_j/\beta_j) d_j^2 2^{j-p} n_0 g_0 Z_0}{Z_0 \lambda - (\alpha_j/\beta_j) d_j^2 2^{j-p}}. \quad (59)$$

Let us now consider a tapered GRIN medium with a divergent linear taper function given by

$$g(z) = \frac{g_0}{1 + z/L}, \quad (60)$$

where L is the distance from $z = 0$ to the common apex of the equi-index lines of the refractive-index profile [10].

When a Walsh function located at the input of this tapered GRIN medium is illuminated by uniform wave (cylindrical wavefront), the axial location of the fractional Talbot images becomes

$$z_{\alpha_j/\beta_j} = L \left\{ \exp \left[\frac{1}{g_0 L} \tan^{-1} \left(\frac{(\alpha_j/\beta_j) d_j^2 2^{j-p} n_0 g_0 Z_0}{Z_0 \lambda - (\alpha_j/\beta_j) d_j^2 2^{j-p}} \right) - 1 \right] \right\}, \quad (61)$$

for the Rademacher function $R_j(x_0)$, and

$$z_{\alpha/\beta} = L \left(\exp \left\{ \frac{1}{g_0 L} \tan^{-1} \left[\frac{(\alpha/\beta) d_p^2 n_0 g_0 Z_0}{Z_0 \lambda - (\alpha/\beta) d_p^2} \right] - 1 \right\} \right), \quad (62)$$

Table 1. Correspondence between different orders of the fractional self-images of $W_{896}(x_0)$ considering fractions of $1/8$, and the fractional self-images orders of its Rademacher functions $R_7(x_0)$, $R_8(x_0)$ and $R_9(x_0)$, calculated using equation (42). The column number represents the order of appearance of the self-images throughout the optical axe since $z = 0$.

Column number:	1	2	3	4	5	6	7	8	9	10	11	12	13	14	15	16
$W_{896} : \frac{\alpha}{\beta} =$	$\frac{1}{8}$	$\frac{1}{4}$	$\frac{3}{8}$	$\frac{1}{2}$	$\frac{5}{8}$	$\frac{3}{4}$	$\frac{7}{8}$	1	$\frac{9}{8}$	$\frac{5}{4}$	$\frac{11}{8}$	$\frac{3}{2}$	$\frac{13}{8}$	$\frac{7}{4}$	$\frac{15}{8}$	2
$R_7 : \frac{\alpha_7}{\beta_7} =$	$\frac{1}{8}$	$\frac{1}{4}$	$\frac{3}{8}$	$\frac{1}{2}$	$\frac{5}{8}$	$\frac{3}{4}$	$\frac{7}{8}$	1	$\frac{9}{8}$	$\frac{5}{4}$	$\frac{11}{8}$	$\frac{3}{2}$	$\frac{13}{8}$	$\frac{7}{4}$	$\frac{15}{8}$	2
$R_8 : \frac{\alpha_8}{\beta_8} =$	$\frac{1}{4}$	$\frac{1}{2}$	$\frac{3}{4}$	1	$\frac{5}{4}$	$\frac{3}{2}$	$\frac{7}{4}$	2	$\frac{9}{4}$	$\frac{5}{2}$	$\frac{11}{4}$	3	$\frac{13}{4}$	$\frac{7}{2}$	$\frac{15}{4}$	4
$R_9 : \frac{\alpha_9}{\beta_9} =$	$\frac{1}{2}$	1	$\frac{3}{2}$	2	$\frac{5}{2}$	3	$\frac{7}{2}$	4	$\frac{9}{2}$	5	$\frac{11}{2}$	6	$\frac{13}{2}$	7	$\frac{15}{2}$	8

for the Walsh function $W_N(x_0)$ [and $R_p(x_0)$] where equations (41), (51), and (59) to (60) have been used.

Using equation (62) we evaluate the distances $z_{\alpha/\beta}$ corresponding to the fractional self-images orders of $W_{896}(x_0)$ in table 1, and the results are shown in figure 3. This plot and these distances $z_{\alpha/\beta}$ correspond also to any Walsh function with $p = 7$, e.g., $W_{128}(x_0) = R_7(x_0)$, $W_{640}(x_0) = R_7(x_0)R_9(x_0)$, $W_{1664}(x_0) = R_7(x_0)R_9(x_0)R_{10}(x_0)$, etc., because the self-image distances $z_{\alpha/\beta}$ depend on the period d_p of the Rademacher function $R_p(x_0)$ of lowest index in the definition of the Walsh function [see, for instance, equations (36), (39), and (62)].

Figure 4 depicts the fractional self-images distances for different Walsh functions, with $p = 6$, $p = 7$, $p = 8$, and $p = 9$, which obey the condition of equation (19). The interval between consecutive Talbot images decreases as p increases, and for a given α/β , the position of fractional Talbot images decreases as p increases.

8. Walsh functions like a complete set of functions

Let us now consider two Walsh functions $W_N(x_0)$ and $W_{N'}(x_0)$. From equations (4) and (39), it follows that the fractional Talbot images of both functions are related by

$$\frac{\alpha'}{\beta'} = \frac{\alpha}{\beta} 4^{p'-p}, \quad (63)$$

where p is the lowest index of the Rademacher functions in the definition of $W_N(x_0)$, and p' is the lowest index of the Rademacher functions in the definition of $W_{N'}(x_0)$. Equation (63) for integer images becomes

$$v' = v 4^{p'-p}. \quad (64)$$

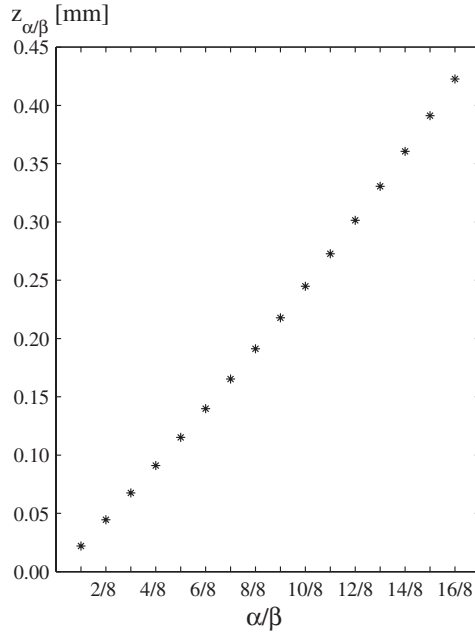


Figure 3. Axial position of fractional self-images of $W_{896}(x_0)$ versus self-image number for a tapered GRIN medium. Calculations have been made for $n_0 = 1.5$, $g_0 = 0.01$, $d_p = 9 \mu\text{m}$, $\lambda = 0.7 \mu\text{m}$, $L = 1 \text{ mm}$, $Z_0 = 15 \text{ mm}$, and $\beta = 8$.

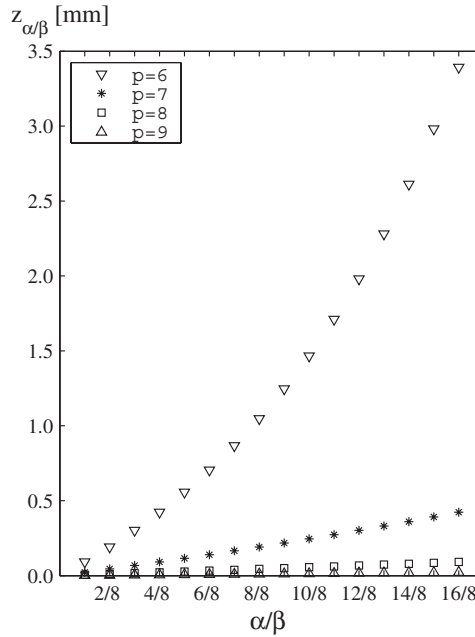


Figure 4. Axial position of fractional self-images versus self-image number for a tapered GRIN medium taken as aperture Walsh functions of $p = 6, 7, 8$ and 9 . Calculations have been made for $n_0 = 1.5$, $g_0 = 0.01$, $\beta = 8$, $\lambda = 0.7 \mu\text{m}$, $L = 1 \text{ mm}$, and $Z_0 = 15 \text{ mm}$, $d_p = (18, 9, 4.5 \text{ and } 2.25) \mu\text{m}$.

If $p' > p$, the integer images of $W_N(x_0)$ coincide with positive integer images of $W_{N'}(x_0)$.

The above results can be extended to a linear combination of both Walsh functions, that is

$$h(x_0) = a_N W_N(x_0) + a_{N'} W_{N'}(x_0), \quad (65)$$

where a_N and $a_{N'}$ are real coefficients. Since integer self-images of $W_N(x_0)$ coincide with positive integer self-images of $W_{N'}(x_0)$, in the places where $W_N(x_0)$ has positive integer self-images the linear combination $h(x_0)$ will have a positive integer self-image as well. The Talbot distance of $h(x_0)$ is then the same as $W_N(x_0)$ and the positive integer self-image of order ν (even) of $W_N(x_0)$ coincides in the same z position with the positive self-image of order ν of $h(x_0)$, therefore we can say that $W_N(x_0)$ governs the positive integer self-image behavior of $h(x_0)$. However, in locations where $W_N(x_0)$ has negative integer self-images, $W_{N'}(x_0)$ has positive integer self-images, the diffracted field at these locations is then not a negative integer self-image of $h(x_0)$. In general, the field at z will be given by a linear superposition of fractional images of $W_N(x_0)$ and $W_{N'}(x_0)$ [whose orders α/β can be calculated by equation (39)].

Finally, considering that Walsh functions constitute a complete set, an arbitrary input function can be expressed as

$$f(x_0) = \sum_{N=0}^{\infty} a_N W_N(x_0). \quad (66)$$

For the set of Walsh functions that contribute to the summation of equation (66) there is a Walsh function or a group of these functions for which the lowest index of their Rademacher functions is smaller than the lowest indices of the remainder functions. Let us call $[W_{\{N\}}(x_0); p]$ this subset. From equation (63) it follows that, where this set of Walsh functions has integer self-images the rest of Walsh functions in equation (66) will have positive integer self-images.

In particular, in locations where the set $[W_{\{N\}}(x_0); p]$ has integer positive self-images all the Walsh functions in equation (66) will have integer positive self-images, in this case the input signal $f(x_0)$ will have an integer positive self-image too. Moreover, where $[W_{\{N\}}(x_0); p]$ has an integer positive self-image of order ν , $f(x_0)$ will have an integer positive self-image of the same order. Therefore we can say that $[W_{\{N\}}(x_0); p]$ governs the positive integer self-image behavior of $f(x_0)$.

9. Conclusions

The light propagation through a tapered gradient-index medium with a binary Walsh function at the input face has been analysed under a nonuniform illumination. We have obtained the integer and fractional self-image conditions for every Rademacher function included in a Walsh function. Furthermore, we have found the integer and fractional self-image conditions for the Walsh function and their dependence on the Rademacher function of lowest index. Moreover, in the same manner that a Walsh function is a product of Rademacher functions, we have demonstrated that its fractional self-images are products of fractional self-images of its Rademacher functions. Mathematical expressions for any fractional Talbot

distance and its evolution along the GRIN medium have been reported. Finally, we have generalized the results to arbitrary functions.

Acknowledgments

This work was supported by the Spanish Ministry of Science and Technology, under contract TIC 99-0489. The fellowship of O. Trabocchi at the University of Santiago de Compostela from the Spanish Ministry of Education, Culture and Sport is gratefully acknowledged.

References

- [1] PATORSKI, K., 1989, *Progress in Optics*, edited by E. Wolf (Amsterdam: North-Holland), Vol. XXVII, pp. 3–101.
- [2] BERRY, M. V., and KLEIN, S., 1996, *J. Mod. Optics*, **43**, 2139.
- [3] FLORES-ARIAS, M. T., BAO, C., PÉREZ, M. V., and GÓMEZ-REINO, C., 1999, *J. Opt. Soc. Am. A*, **16**, 2439.
- [4] FLORES-ARIAS, M. T., FERNÁNDEZ-POUSA, C. R., PÉREZ, M. V., BAO, C., and GÓMEZ-REINO, C., 2000, *J. Opt. Soc. Am. A*, **17**, 1007.
- [5] BEAUCHAMP, K. G., 1975, *Walsh Functions and their Applications* (New York: Academic Press).
- [6] TRABOCCHI, O., COLAUTTI, C., and SICRE, E. E., 1996, *Opt. Eng.*, **35**, 94.
- [7] TRABOCCHI, O., COLAUTTI, C., and SICRE, E. E., 1997, *J. Mod. Optics*, **44**, 715.
- [8] COLAUTTI, C., RUIZ, B., SICRE, E. E., and GARAVAGLIA, M., 1987, *J. Mod. Optics*, **34**, 1385.
- [9] BLACHMAN, N. M., 1974, Sinusoids versus Walsh Functions. In *Proceedings of the IEEE*, **62**, pp. 346–354.
- [10] GÓMEZ-REINO, C., PÉREZ, M. V., and BAO, C., 2002, *Gradient-Index Optics: Fundamentals and Applications* (Berlin: Springer-Verlag), Chaps. 1 and 2.